Eph-B4 prevents venous adaptive remodeling in the adult arterial environment

Akihito Muto,[1,2] Tai Yi,[2] Kenneth D. Harrison,[2] Alberto Dávalos,[2] Tiffany T. Fancher,[3] Kenneth R. Ziegler,[1,2] Amanda Feigel,[1,2] Yuka Kondo,[1,2] Toshiya Nishibe,[4] William C. Sessa,[2] and Alan Dardik[1,2,5]

[1]Department of Surgery and [2]Department of Vascular Biology and Therapeutics Program, Yale University School of Medicine, New Haven, CT 06520
[3]Saint Mary's Hospital, Waterbury, CT 06706
[4]Tokyo Medical University Hachioji Medical Center, Hachioji, Tokyo 193-0998, Japan
[5]VA Connecticut Healthcare System, West Haven, CT 06515

Eph-B4 determines mammalian venous differentiation in the embryo but is thought to be a quiescent marker of adult veins. We have previously shown that surgical transposition of a vein into the arterial environment is characterized by loss of venous identity, as indicated by the loss of Eph-B4, and intimal thickening. We used a mouse model of vein graft implantation to test the hypothesis that Eph-B4 is a critical determinant of venous wall thickness during postsurgical adaptation to the arterial environment. We show that stimulation of Eph-B4 signaling, either via ligand stimulation or expression of a constitutively active Eph-B4, inhibits venous wall thickening and preserves venous identity; conversely, reduction of Eph-B4 signaling is associated with increased venous wall thickness. Stimulated Eph-B4 associates with caveolin-1 (Cav-1); loss of Cav-1 or Eph-B4 kinase function abolishes inhibition of vein graft thickening. These results show that Eph-B4 is active in adult veins and regulates venous remodeling. Eph-B4–Cav-1–mediated vessel remodeling may be a venous-specific adaptive mechanism. Controlled stimulation of embryonic signaling pathways such as Eph-B4 may be a novel strategy to manipulate venous wall remodeling in adults.

CORRESPONDENCE
Alan Dardik:
alan.dardik@yale.edu

Abbreviations: Cav-1, caveolin 1; EC, endothelial cell; MLEC, mouse lung EC; RTK, receptor tyrosine kinase.

Veins are thin-walled blood vessels suited to low shear stress and high capacitance blood flow and are both structurally and molecularly distinct from arteries. Venous specification in the embryo was recently demonstrated to be regulated by COUP-TFII repression of Notch signaling, with subsequent failure to induce expression of the arterial determinant Ephrin-B2 and allowance of expression of Eph-B4 (You et al., 2005). Eph-B4, a member of the Eph receptor tyrosine kinase (RTK) family, has been described as a marker of venous endothelial cell (EC) determination in embryonic development of diverse species including mouse, chick, zebrafish, and *Xenopus laevis* (Adams et al., 1999). Although Eph-B4 is an active determinant of embryonic venous development (Wang et al., 1998; Adams et al., 1999; Gerety et al., 1999; Shin et al., 2001), and Eph-B4 is present in adult veins, giving the vein a marker of identity, the function of Eph-B4 in adult veins is currently unknown. Eph-B4 function in adult cells has been previously associated with

pathological functions such as angiogenesis and tumorogenesis (Erber et al., 2006; Foo et al., 2006; Foubert et al., 2007). As such, it is unclear whether there is basal Eph-B4 function in normal adult veins.

Cardiovascular disease remains the leading cause of death worldwide. Mortality and morbidity are most frequently a result of atherosclerosis in which focal arterial stenoses and occlusions manifest as both acute and chronic ischemia. Veins are frequently used for surgical therapy to bypass focal arterial lesions, both in the heart and the periphery. In particular, veins are the most commonly placed conduit in peripheral vascular surgery and are the gold standard for long-term clinical performance (Veith et al., 1986). Similarly, despite the common use of the internal mammary artery for coronary
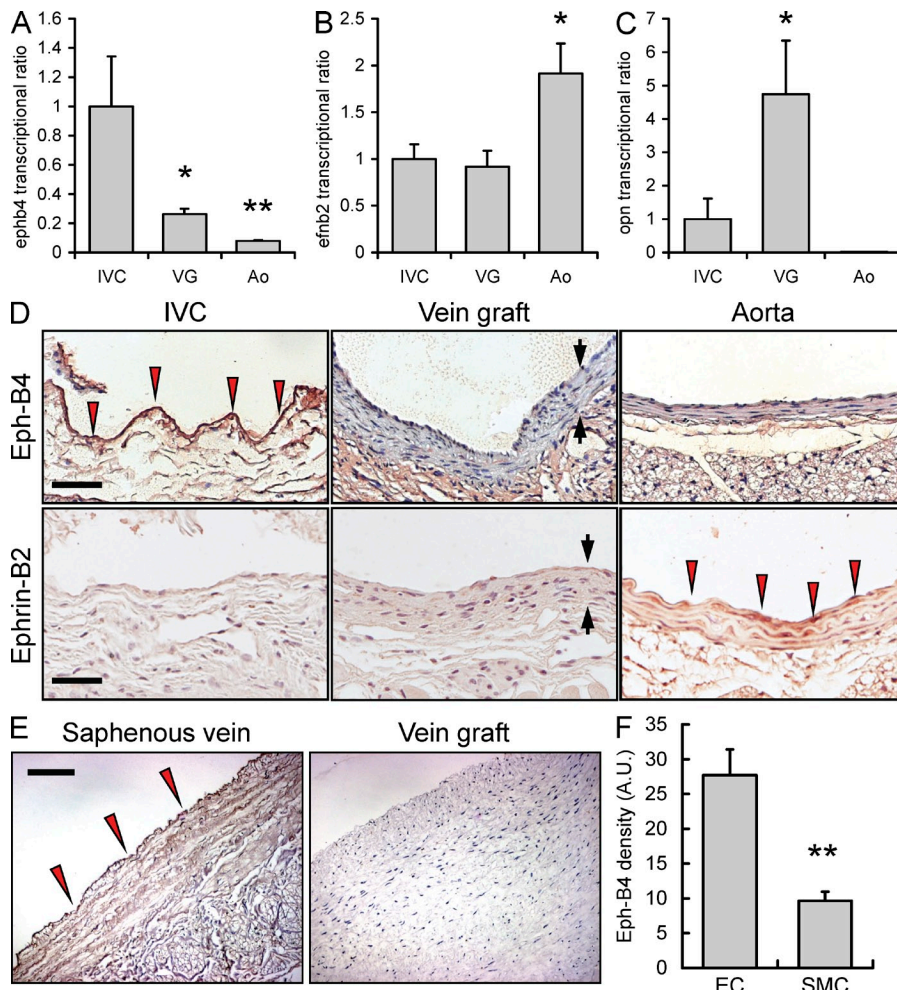
Figure 1. Venous expression of Eph–B4 during vein graft adaptation in both a mouse model and in human specimens. (A–C) Expression of *ephb4* (A), *efnb2* (B), and *opn* mRNA (C). *n* = 4. IVC, inferior vena cava; VG, vein graft; Ao, aorta. Error bars denote SEM. (D) Eph-B4 and Ephrin-B2 immunoreactivity at 3 wk of vein graft adaptation in mice. Photomicrographs show representative samples from *n* = 4 independent samples for each group. Bars, 100 µm. Black arrows show the vein graft wall. Red arrowheads indicate Eph-B4– and Ephrin-B2–positive signals. (E) Eph-B4 immunoreactivity during human vein graft adaptation. Representative photomicrographs from two independent samples are shown. Bar, 250 µm. Red arrowheads point to the Eph-B4–positive signal. (F) Distribution of Eph-B4 in mouse veins (*n* = 4) as determined by immunofluorescence. The density of cells immunoreactive for both Eph-B4 and either CD31 or α-actin was analyzed by ImageJ (National Institutes of Health). **, P < 0.01; *, P < 0.05. Error bars denote SEM.

artery bypass, vein grafts continue to demonstrate superior long-term outcomes and function compared with radial artery grafts (Desai et al., 2004; Khot et al., 2004). Nevertheless, the response of veins transposed to the arterial environment remains poorly characterized (Kudo et al., 2007).

Venous adaptation to the arterial environment is characterized by thickening of the venous intima, media, and adventitia, resulting from deposition of smooth muscle cells and extracellular matrix components, stimulating remodeling and reduced compliance by mechanisms that are thought to be similar to those active after arterial injury and that result in neointimal hyperplasia (Owens et al., 2006, 2008; Kudo et al., 2007). In particular, Owens et al. (2006, 2008) recently demonstrated positive remodeling, e.g., increased diameter and wall thickness, in clinically successful human vein grafts with high resolution imaging. However, it is not currently understood which aspects of remodeling are critical for successful vein graft function in an arterial environment. It is also not known to what extent wall thickening is adaptive and at what point the remodeling and thickening becomes pathological or even how excessive thickening might contribute to vein graft failure. The disappointing failure of the PREVENT-III and PREVENT-IV trials show that strategies to prevent vein

graft failure that focus on inhibition of smooth muscle cell proliferation are not likely to be clinically useful (Alexander et al., 2005; Conte et al., 2006).

To examine the function of veins successfully transplanted into the arterial environment, we previously determined the response of the jugular vein transposed into the rat carotid artery. This model showed that decreased expression of Eph-B4 is associated with intimal thickening (Kudo et al., 2007). These results suggest that Eph-B4 actively maintains adult venous identity by responding to the ambient environment, limiting venous wall thickness. A corollary to this proposition is the hypothesis that surgical transposition of a vein to the arterial environment results in loss of Eph-B4 and venous identity and, with this loss of negative inhibition, subsequent alteration of venous structure and function. To test this hypothesis, we developed a surgical model of vein graft adaptation in mice and examined the effects and mechanisms of altered Eph-B4 signaling on vein graft thickening and identity.

RESULTS

Reduced Eph–B4 during mouse and human vein graft adaptation

To establish a model of vein graft adaptation, we determined the time course of morphological and physiological changes in veins implanted into allogeneic C57BL/6 mice. The suprahepatic inferior vena cava was transplanted from a donor mouse into the infrarenal aorta of a recipient mouse. Laminar flow
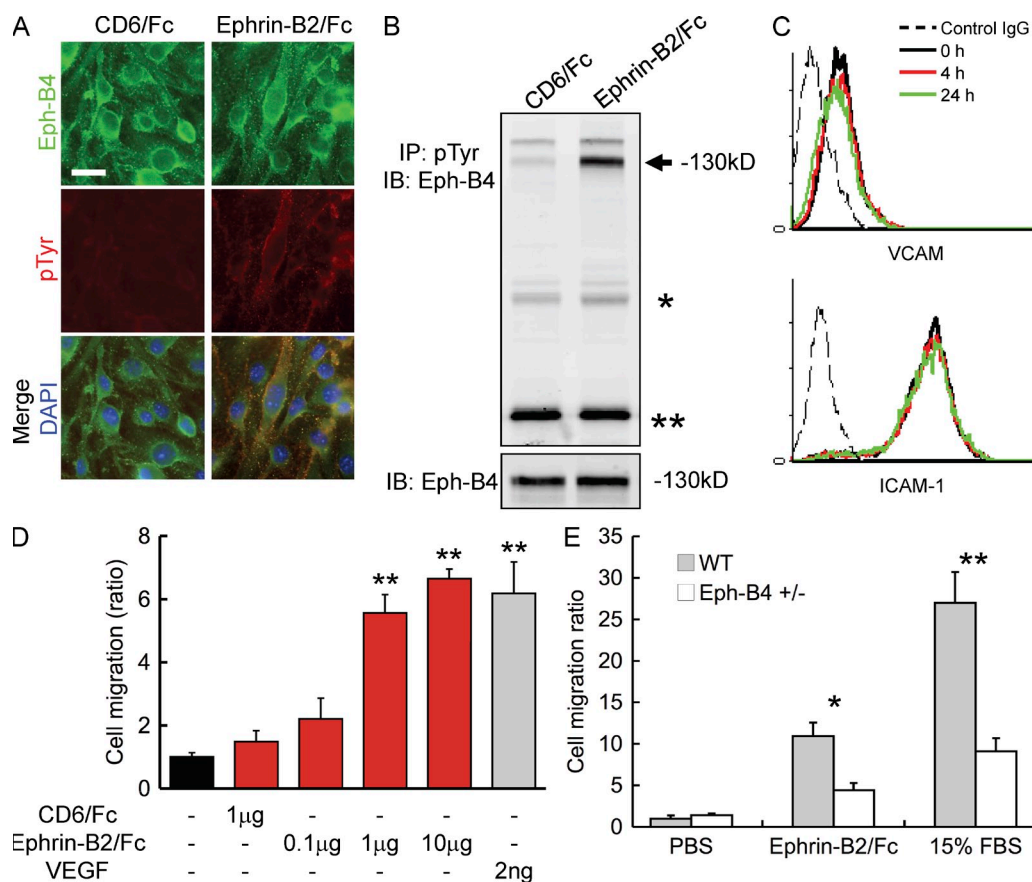
Figure 2.   Recombinant Ephrin–B2/human IgG Fc chimeric protein activates the Eph–B4 receptor in vitro. (A) EC expression of Eph-B4 (green), phosphotyrosine (red), or both (merge) after 5 min of treatment with 2 µg/ml of control CD6/Fc or 2 µg/ml Ephrin-B2/Fc. Bar, 50 µm. (B) Immunoprecipitation analysis of tyrosine-phosphorylated Eph-B4 (arrowhead) in EC treated with Ephrin-B2/Fc. *, IgG heavy chain; **, IgG light chain. Bottom shows total cell lysate. (C) Expression of VCAM and ICAM on EC treated with Ephrin-B2/Fc. $n = 3$. (D) Migration of WT EC in response to Ephrin-B2/Fc, control CD6/Fc, or VEGF. $n = 3$. Error bars denote SEM. (E) Migration of WT or Eph-B4$^{+/-}$ EC in response to Ephrin-B2/Fc or FBS. $n = 3$. **, $P < 0.01$; *, $P < 0.05$. Error bars denote SEM.

was preserved by suturing the anastomoses in standard micro-surgical fashion and confirmed by ultrasonography. Vein graft wall thickness increased in a time-dependent manner, with increased wall thickness up to 6 wk after implantation (Fig. S1). Serial observations of vein grafts using ultrasound imaging showed that increased vein graft wall thickness and reduced compliance reach a plateau at 4–6 wk, with only a small amount of positive remodeling until 8 wk (Fig. S1 F). Surprisingly, vein grafts showed some late positive remodeling by 12 wk, consistent with results of late dilation and aneurysmal degeneration in long-standing functional human vein grafts (Szilagyi et al., 1973; Loftus et al., 1999). Therefore, the mouse vein graft model closely mimics early human vein graft adaptation, at least until 3–4 wk (Owens et al., 2006, 2008).

We have previously demonstrated decreased Eph-B4 gene expression, without increased Ephrin-B2 gene expression, in a rat model of vein graft adaptation (Kudo et al., 2007). Mouse vein grafts also showed decreased Eph-B4 gene expression and no change in Ephrin-B2 expression (Fig. 1, A and B). As expected, mouse vein grafts showed increased osteopontin

gene expression, a marker of vein graft adaptation (Abeles et al., 2006; Fig. 1 C). Similarly, there was diminished Eph-B4 protein in all layers of mouse vein grafts compared with strong detection in veins, and there was no increased detectable Ephrin-B2 protein in the mouse vein grafts wall (Fig. 1 D). Diminished Eph-B4 protein in vein grafts was a pattern also found in patent human vein grafts (Fig. 1 E). To identify the distribution of Eph-B4 immunoreactivity within the native vein wall, we analyzed the relative distribution of Eph-B4 in ECs and smooth muscle cells of both abdominal and thoracic mouse inferior vena cava (Fig. 1 F). Eph-B4 was distributed predominantly on ECs, with ECs showing three times more immunoreactivity compared with smooth muscle cells, with a similar ratio in the thoracic and abdominal vena cavae (un-published data).

Eph–B4 is active and limits wall thickness in adult veins

Diminished Eph-B4 expression without induction of Ephrin-B2 expression is consistent with our hypothesis that Eph-B4 actively limits venous wall thickness in adult veins, and
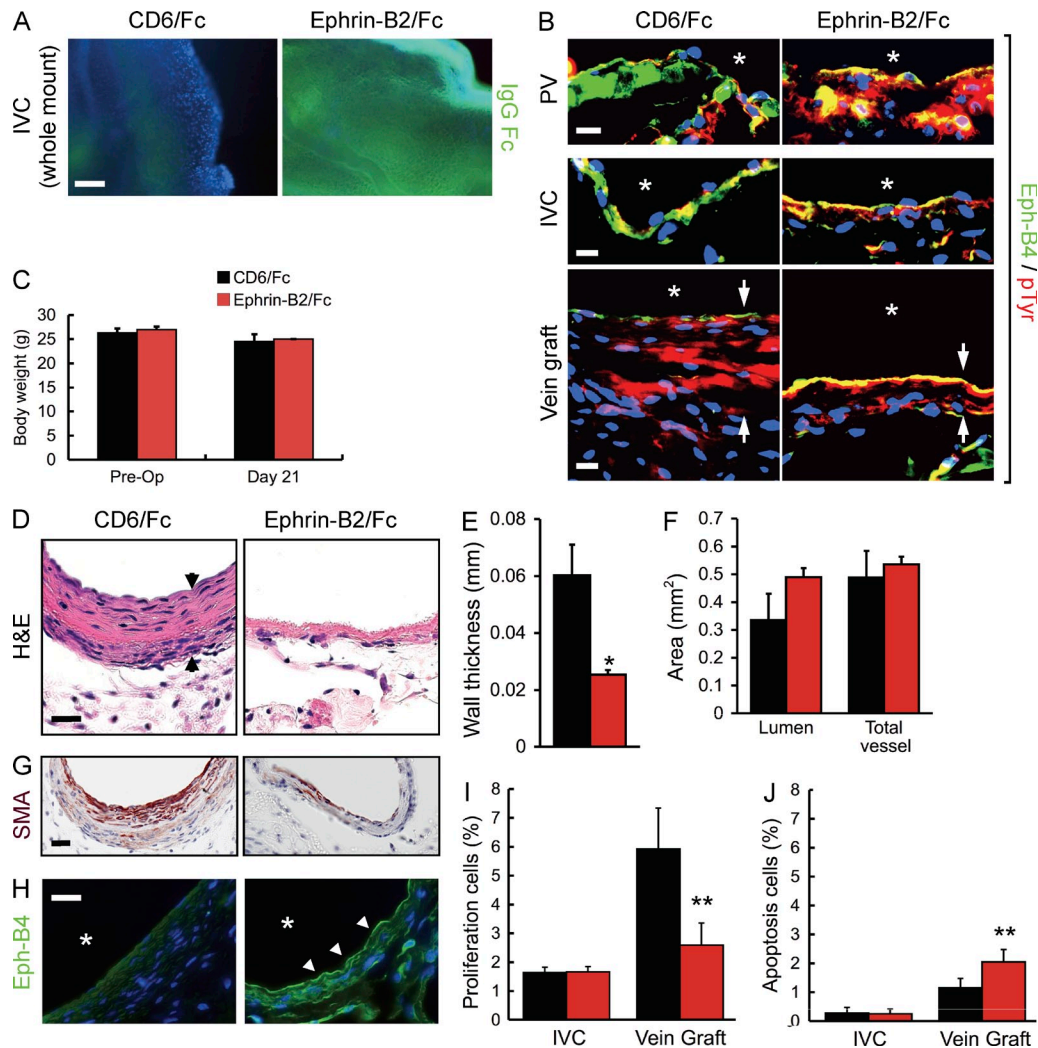
Figure 3. Ephrin–B2/Fc activates Eph–B4 and decreases vein graft wall thickness in vivo. (A) Immunofluorescence of anti–human IgG-FITC in whole mount inferior vena cava (IVC) isolated from mice 24 h after injection with control CD6/Fc or Ephrin-B2/Fc. Representative photomicrographs from three independent samples are shown. Bar, 20 µm. (B) Expression of Eph-B4 (green), phosphotyrosine (red), or both (merge) in pulmonary vein (PV), inferior vena cava, or vein graft (VG) of mice after 3 wk of treatment with control CD6/Fc or Ephrin-B2/Fc. Representative photomicrographs from three independent samples are shown. Star indicates vessel lumen. Arrows show vein graft wall. Bars, 20 µm. pTyr, phosphotyrosine. (C) Mouse body weight during treatment with control CD6/Fc or Ephrin-B2/Fc. Error bars denote SEM. (D, G, and H) Mouse vein grafts after 3 wk of treatment with control CD6/Fc or Ephrin-B2/Fc, examined with H&E staining (D), immunoreactivity against α-actin (SMA; G), or immunofluorescence against Eph-B4 (H). Arrowheads show vein graft wall. *, lumen. Bars, 20 µm. (E and F) Vein graft wall thickness and lumen/total vessel area after control CD6/Fc or Ephrin-B2/Fc treatment. Error bars denote SEM. (I and J) Percentage of cells in the walls of the inferior vena cava or vein grafts, treated with control CD6/Fc or Ephrin-B2/Fc and positively staining for proliferation (I) or apoptosis (J). Error bars denote SEM. All experiments analyzed five (CD6/Fc) and seven (Ephrin-B2/Fc) mice. *, P < 0.05; **, P < 0.01.

diminished Eph-B4 expression during vein graft adaptation allows increased wall thickness. To confirm this hypothesis, we examined vein grafts with both increased and reduced Eph-B4 signaling. To determine the response of veins implanted into the arterial environment, but with increased Eph-B4 signaling, Eph-B4 signaling was first stimulated with its soluble ligand Ephrin-B2/Fc. Consistent with previous studies and as expected, Ephrin-B2/Fc induces Eph-B4 phosphorylation in venous ECs in vitro (Fig. 2, A and B), without induction of a dysfunctional endothelial phenotype (Fig. 2 C). In addition, Ephrin-B2/Fc also stimulates migration in a dose-dependent manner in WT EC (Fig. 2 D) with reduced migration in Eph-B4^{+/−}–derived EC (Fig. 2 E). Stimulation of migration in WT venous EC is consistent with the EC being Eph-B4 positive and Ephrin-B2 negative, as previously reported (Steinle et al., 2002).

We hypothesized that stimulation of Eph-B4 signaling in veins transplanted to the arterial environment would promote retention of Eph-B4, preventing venous intimal thickening with maintenance of venous thin–wall architecture. To stimulate Eph-B4 in surgically implanted vein grafts, Ephrin-B2/Fc was injected intraperitoneally from the day before surgical implantation and then every other day after surgical vein graft
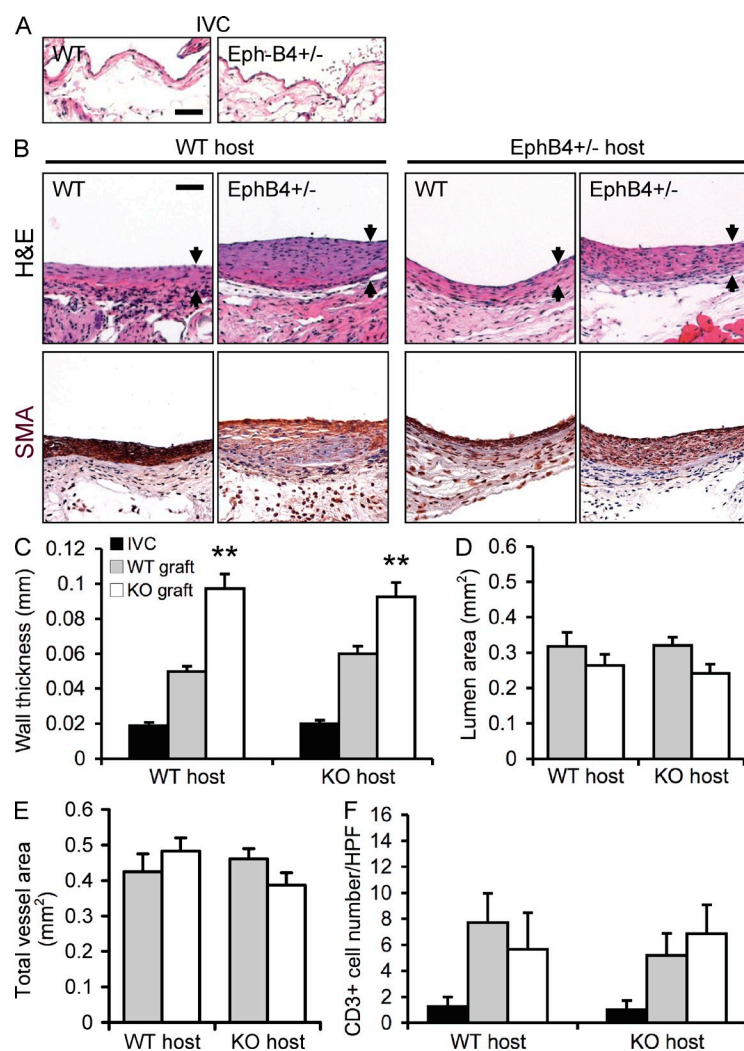
Figure 4.   Increased intimal thickening in vein grafts derived from Eph–B4$^{+/-}$ mice (4 wk). (A) Histology of veins derived from WT (WT) or Eph-B4 heterozygous KO (Eph-B4$^{+/-}$) mice stained with H&E. Bar, 50 µm. (B) Morphology of vein graft adaptation of WT or Eph-B4$^{+/-}$ vein grafts placed into WT or Eph-B4$^{+/-}$ hosts, examined with H&E staining or smooth muscle α-actin (SMA) immunoreactivity. Arrows show intimal thickening. Bar, 100 µm. (C–E) Vein and vein graft wall thickness (C), vein graft lumen area (D), and total vein graft area (E). Error bars denote SEM. (F) Numbers of CD3 immunoreactive cells infiltrated into veins and vein grafts. Error bars denote SEM. n = 5–7 in each group. **, P < 0.01.

with retention of venous identity. In addition, vein grafts derived from Ephrin-B2/Fc–injected mice showed increased colocalization of Eph-B4 and phosphotyrosine in the endothelium (Fig. 3 B, bottom), which is consistent both with Ephrin-B2/Fc stimulation of Eph-B4 and retention of Eph-B4 in the endothelium (Fig. 3 H). These vein grafts also showed diminished proliferation and increased apoptosis compared with control vein grafts (Fig. 3, I and J).

It is possible that the Fc moiety of Ephrin-B2/Fc could activate complement or macrophages, providing an alternative mechanism to regulate vein graft wall thickness (Stabila et al., 1998; Tawara et al., 2008). However, there were no differences in complement activation or numbers of infiltrating macrophages in vein grafts derived from control or Ephrin-B2/Fc–injected mice (Fig. S2), suggesting that the thinner vein grafts in Ephrin-B2/Fc–injected mice (Fig. 3, D, E, and G) are mediated by altered Eph-B4 signaling rather than by stimulation of either complement or macrophages.

To show that the remodeling response is intrinsic to the vein graft, and to confirm the hypothesis that reduced Eph-B4 signaling results in thicker vein grafts, we used a genetically modified mouse with reduced Eph-B4 signaling as previously described (Gerety et al., 1999). Homozygous deletion of Eph-B4 is an embryonic lethal phenotype. Heterozygous KO mice (Eph-B4$^{+/-}$) were used as a source of veins with diminished Eph-B4 signaling. Compared with WT veins, veins derived from Eph-B4$^{+/-}$ mice have similar morphology and thickness before implantation as vein grafts (Fig. 4 A). Eph-B4$^{+/-}$ veins implanted into littermate host mice were ~100% thicker than WT veins, with approximately twice as many layers of α-actin–positive cells (Fig. 4, B and C). To confirm that the thickening response was associated with the vein graft, veins derived from littermate or Eph-B4$^{+/-}$ mice were implanted into Eph-B4$^{+/-}$ host mice. These veins showed similar patterns of thickening to those in veins implanted into WT hosts (Fig. 4, B and C), confirming that diminished Eph-B4 signaling in the vein graft promotes vein graft thickening. Despite increased wall thickness in vein grafts derived from Eph-B4$^{+/-}$ mice, lumen encroachment and outward vessel remodeling did not achieve significance

implantation until vein graft harvest, as previously described (Noren et al., 2006). 24 h after intraperitoneal injection, Ephrin-B2/Fc, but not control CD6/Fc, was detectable in veins, confirming its in vivo localization to Eph-B4–positive tissue (Fig. 3 A, right, green) and, therefore, its suitability to stimulate Eph-B4 signaling in vein grafts. 3 wk after injection, there was increased colocalization of Eph-B4 and phosphotyrosine in pulmonary EC as well as EC lining the inferior vena cava, suggesting increased Eph-B4 pathway phosphorylation after administration of Ephrin-B2/Fc in vivo (Fig. 3 B, top and middle). Despite 3 wk of Ephrin-B2/Fc treatment, mice did not suffer any adverse clinical events; mean body weight was unchanged compared with control mice (Fig. 3 C). Notably, after Ephrin-B2/Fc treatment, vein grafts showed reduced wall thickness and reduced numbers of layers of α-actin–positive cells compared with control (CD6/Fc injected) vein grafts (Fig. 3, D, E, and G). Although control vein grafts showed diminished Eph-B4 expression and loss of venous identity in the arterial environment, as previously shown (Fig. 1, A and D), vein grafts derived from Ephrin-B2/Fc–injected mice showed retention of Eph-B4 expression (Fig. 3 H), which is consistent
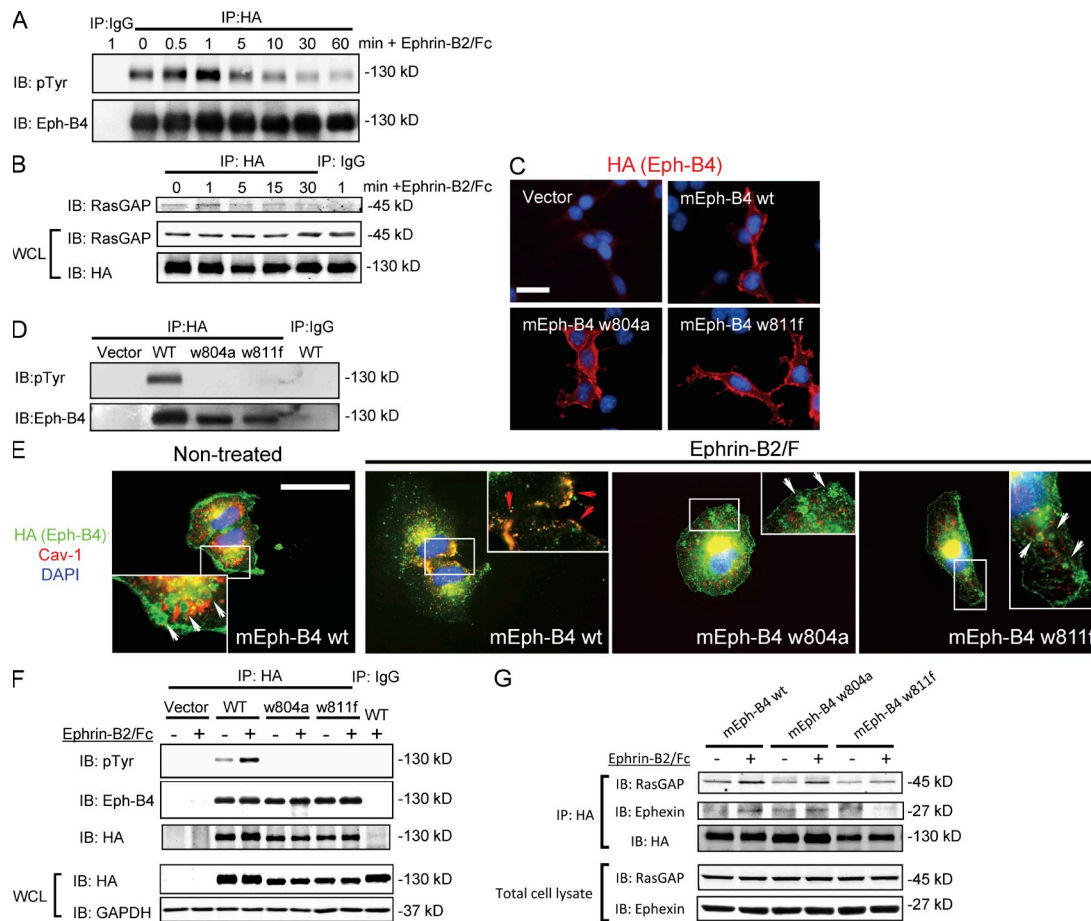
Figure 5. Plasmids with mutated Eph–B4 kinase domain have defective Eph–B4 phosphorylation. (A) Time course of Eph-B4 phosphorylation, stimulated with 2 µg/ml Ephrin-B2/Fc, in HEK293 cells transfected with HA-tagged mEph-B4 plasmid. (B) Time course of Ras-GAP association with Eph-B4, stimulated with 2 µg/ml Ephrin-B2/Fc, in HEK293 cells transfected with HA-tagged mEph-B4 plasmid. (C) Immunofluorescence for HA-tagged Eph-B4 in HEK293 cells transfected with either mEph-B4 wt plasmid or mutant (w804a and w811f) mEphB4 plasmids, counterstained with DAPI. Bar, 50 µm. (D) Tyrosine phosphorylation in response to Ephrin-B2/Fc in HEK293 cells transfected with WT or mutant (w804a and w811f) mEph-B4 plasmids. (E) Immuno-fluorescence of HA-tagged Eph-B4 (green), cav-1 (red), or merge (yellow) in COS cells transfected with WT or mutant Eph-B4 plasmids, counterstained with DAPI, and without or with stimulation with Ephrin-B2/Fc. White arrowheads show Eph-B4 in the intracellular vesicles. Red arrowheads show colocalization of Eph-B4 with cav-1 at the cell membrane, after treatment with Ephrin-B2/Fc, in WT but not mutant Eph-B4 plasmids. Bar, 100 µm. (F) Tyrosine phosphorylation in response to Ephrin-B2/Fc in COS cells transfected with WT or mutant (w804a, w811f) mEph-B4 plasmids. (G) Ras-GAP or Ephexin association with Eph-B4, stimulated with 2 µg/ml Ephrin-B2/Fc, in COS cells transfected with HA-tagged mEph-B4 plasmid. All panels show representative samples from three independent experiments. WCL, whole cell lysate.

(Fig. 4, D and E). There were no significant differences in CD3^{+} infiltrating cells in any of the vein grafts, demonstrating that the thickened Eph-B4^{+/−}–derived vein grafts were not a result of T cell–mediated responses (Fig. 4 F). These results are consistent with our hypothesis that Eph-B4 is active in adult veins and plays a role in limiting vein graft wall thickness during vein graft adaptation.

Eph-B4 phosphorylation is a critical determinant of venous adaptation to the arterial environment

To test the importance of Eph-B4 function during vein graft adaptation, we mutated a single site in the kinase domain of the Eph-B4 receptor, which has the conserved consensus sequence WSYGIVMW at residues 804–811 in mice, either from tryptophan to alanine (site 804) or to phenylalanine (site 811).

These residues in the kinase domain have been reported to be an important for the catalytic role of RTK (García-Cardeña et al., 1997; Nystrom et al., 1999; Abulrob et al., 2004; Vihanto et al., 2006). Transfection of WT Eph-B4 plasmid DNA into HEK293 cells showed time-dependent Eph-B4 tyrosine phosphorylation in response to Ephrin-B2/Fc (Fig. 5 A) as well as time-dependent association with the downstream effector RasGAP (Fig. 5 B). Transfection of cells with either WT or mutant plasmids expressing a single amino acid substitution in Eph-B4 (w804a or w811f; Vihanto et al., 2006) resulted in expression of Eph-B4 at the cell membrane (Fig. 5 C) and intracellular vesicles (Fig. 5 E, arrowheads). Although both WT and mutant Eph-B4 were expressed at the cell membrane, only WT Eph-B4 colocalized with Cav-1 after treatment with Ephrin-B2/Fc (Fig. 5, C and E). HEK293
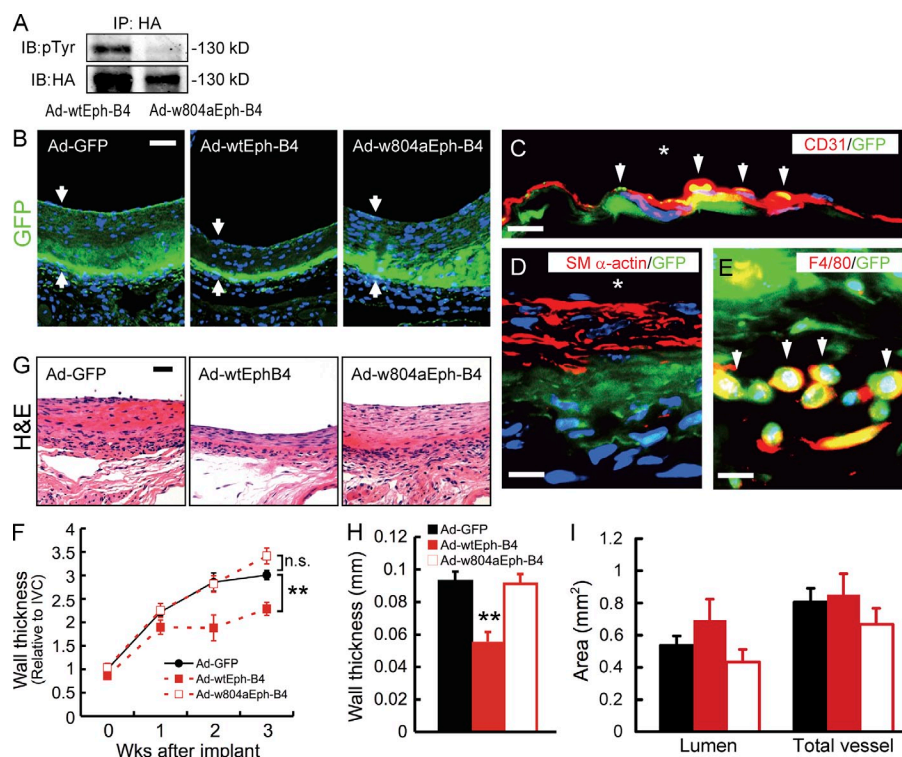
Figure 6. **Eph-B4 inhibition of vein graft thickening depends on a functional Eph-B4 kinase domain.** (A) Tyrosine phosphorylation on Eph-B4 in EC transfected with Ad-Eph-B4 wt or Ad-Eph-B4 w804a. n = 3. (B and G) Vein grafts, transfected with Ad-GFP, Ad-Eph-B4 wt, or Ad-Eph-B4 w804a, were implanted into WT mice for 3 wk and then examined for GFP immunofluorescence (B) or H&E staining (G). Arrows show vein graft wall. Bars, 50 μm. (C–E) Immunofluorescence of CD31 (red) and GFP (green; C), SM α-actin (red) and GFP (green; D), and F4/80 (red) and GFP (green; E) in Ad-Eph-B4 wt-transfected vein grafts. Bars, 20 μm. Arrowheads show colocalized cells. *, lumen. (F) Vein graft wall thickness as determined by serial ultrasounds in mice. Vein grafts were control grafts (filled circle) or treated with Ad-Eph-B4 wt (filled red square) or Ad-Eph-B4 w804a (empty red square). Error bars denote SEM. (H and I) Vein graft wall thickness, and lumen and total vessel area, after 3 wk, in vein grafts transfected with Ad-GFP, Ad-Eph-B4 wt, or Ad-Eph-B4 w804a. **, P < 0.01. n.s., not significant. Error bars denote SEM. B–I show representative data from n = 6 independent samples.

or COS cells transfected with mutant Eph-B4 showed inability to phosphorylate tyrosine in response to Ephrin-B2/Fc, compared with stimulated tyrosine phosphorylation in cells transfected with WT Eph-B4 (Fig. 5, D and F). Mutant Eph-B4 still retained the ability to bind to downstream effectors RasGAP and Ephexin, similar to WT Eph-B4 (Fig. 5, G), suggesting that the defects in tyrosine phosphorylation in the mutant Eph-B4 are specific. These results suggest that WT Eph-B4 stimulates Eph-B4 phosphorylation and cav-1 colocalization and that mutations of the kinase domain of Eph-B4 fail to phosphorylate tyrosine.

To test this idea during vein graft adaptation, adenoviral vectors were generated from plasmids encoding WT Eph-B4 and the Eph-B4 point mutation w804a. Adenovirus with WT Eph-B4 retained the ability to induce tyrosine phosphorylation in EC in vitro, whereas adenovirus with mutant Eph-B4 w804a did not (Fig. 6 A), which is similar to the activities of the original plasmid (Fig. 5, D and F). Vein grafts were transfected with 1.0×10^9 pfu adenovirus, first applied ex vivo for 20 min before implantation and then with additional treatment to the adventitia in vivo using pluronic gel containing the remainder of the adenovirus (Mann et al., 1999; Alexander et al., 2005; Conte et al., 2006). Adenovirus was present in both the endothelium and the adventitia of both control and Eph-B4–transfected vein grafts (Fig. 6 B). Adenovirus was retained both in endothelium and adventitial macrophages, but not medial smooth muscle cells, in transfected vein grafts (Fig. 6, C–E). Vein grafts transfected with control adenovirus (Ad-GFP) developed wall thickening (Fig. 6, F and G [left]), which was similar to that previously demonstrated (Fig. S1).

Vein grafts transfected with WT Eph-B4–expressing adenovirus (Ad-Eph-B4 wt), e.g., with functional Eph-B4 signaling, showed significantly reduced wall thickness (Fig. 6, F, G [middle], and H), which is similar to the thin vein graft wall seen with Ephrin-B2/Fc treatment (Fig. 3, D and E). These results confirm that stimulation of Eph-B4 signaling prevents wall thickening during vein graft adaptation. Adventitial macrophages may represent a reservoir of adenovirus mediating Eph-B4 function. Vein grafts transfected with the adenovirus coding for mutant Eph-B4 (Ad-Eph-B4 w804a), e.g., without functional Eph-B4 signaling, showed similar wall thickness as control vein grafts (Fig. 6, F, G [right], and H), confirming our results which show that Eph-B4 signaling and function mediate vein graft adaptation (Fig. S5).

Eph-B4 signaling is linked with caveolin-1 (Cav-1)

To determine a mechanism by which Eph-B4 limits vein graft wall thickness during vein graft adaption, we examined Cav-1 function during vein graft adaptation. Cav-1 is a major structural protein of caveolae in EC and is thought to be involved with mechanotransduction of dynamic shear stress changes by interaction with several signaling protein families, including G protein–coupled receptors, eNOS, β1-integrin, Src, Jak-Stat, ERK 1/2, and several RTKs including Eph receptors (Gratton et al., 2004; Yu et al., 2006). We hypothesized that Cav-1 and Eph-B4 interact during vein graft adaptation because Cav-1 interacts with several RTKs (Couet et al., 1997b; Yamamoto et al., 1998; Nystrom et al., 1999; Lajoie et al., 2007) and, in particular, Cav-1 has been shown to be required for Eph-B1 receptor downstream signaling
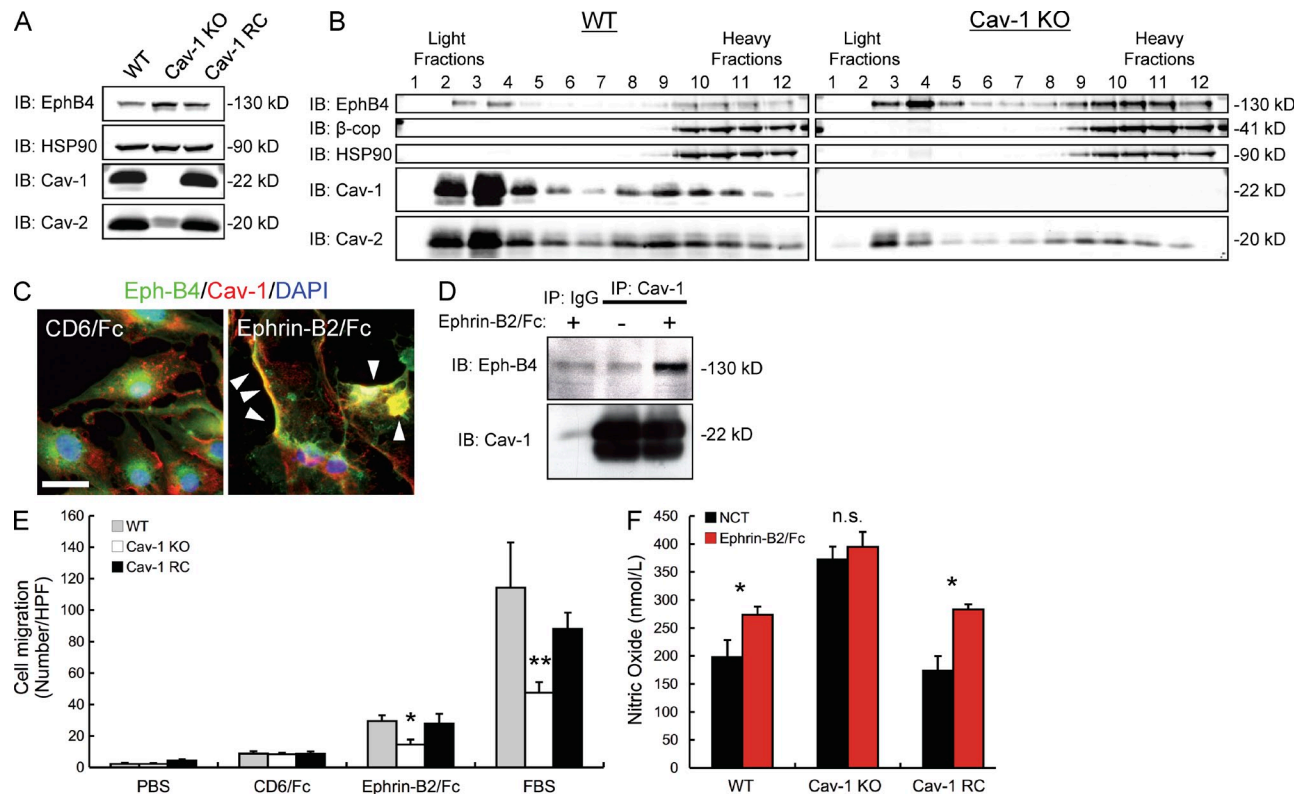
Figure 7. Eph–B4 signaling is linked to Cav–1 in vitro. (A) Eph-B4 expression in ECs derived from WT mice, Cav-1 KO mice, or Cav-1 KO mice with EC-specific reconstitution of Cav-1 (Cav-1 RC). $n = 3$. Bar, 50 µm. (B) Sucrose gradient analysis of WT EC or Cav-1 KO EC. $n = 3$. (C) Immunofluorescence of Eph-B4 (green), cav-1 (red), or both (merge) in EC stimulated with control CD6/Fc or Ephrin-B2/Fc. Arrowheads show colocalization. $n = 3$. (D) Cav-1 association with Eph-B4, stimulated with 2 µg/ml Ephrin-B2/Fc, in EC. $n = 3$. (E) Migration of WT, Cav-1 KO, or Cav-1 RC EC in response to CD6/Fc, Ephrin-B2/Fc, or FBS. $n = 3$. *, $P < 0.05$; **, $P < 0.01$. Error bars denote SEM. (F) Nitric oxide production by WT, Cav-1 KO, or Cav-1 RC EC in response to control or Ephrin-B2/Fc. $n = 3$. *, $P < 0.05$. Error bars denote SEM. NCT, negative control. n.s., not significant.

(Vihanto et al., 2006). In addition, Eph-B4 is predominantly distributed in the venous endothelium (Fig. 1 F), which is in physical proximity to Cav-1. Our experimental results showing increased intimal thickening in vein grafts derived from Eph-B4$^{+/-}$ mice compared with WT mice, despite morphologically similar preimplantation veins (Fig. 5), are consistent with effects of impaired endothelial mechanotransduction in response to transposition to the arterial environment, further suggesting the possibility that Eph-B4 activity may be regulated by Cav-1 (Couet et al., 1997a; Rizzo et al., 1998; Murata et al., 2007).

Eph-B4 is present in EC derived from WT mice, Cav-1 KO mice, and Cav-1 KO mice with EC-specific reconstitution of Cav-1 (Cav-1 RC; Fig. 7 A; Yu et al., 2006; Murata et al., 2007). Sucrose gradient analysis showed cosedimentation of Eph-B4 within the light membrane-enriched fractions in both WT and Cav-1 KO EC (Fig. 7 B). Cosedimentation of Eph-B4 within the light membrane–enriched fractions was not an artifact of EC isolation and culture because Eph-B4 cosedimented with the light membrane–enriched fractions of the original lung tissue in both WT and Cav-1 KO mice (Fig. S3). In WT EC, immunofluorescence showed distinct localization of Eph-B4 (green fluorescence) and Cav-1

(red fluorescence) under basal conditions but colocalization of Eph-B4 with Cav-1 after activation of Eph-B4 with Ephrin-B2/Fc (Fig. 7 C). Similarly, the interaction of Eph-B4 and Cav-1, detected with immunoprecipitation, is enhanced after activation of Eph-B4 with Ephrin-B2/Fc (Fig. 7 D). EC derived from Cav-1 KO mice showed a 50% reduction of Ephrin-B2/Fc–induced migration, compared with WT EC, which was rescued by Cav-1 reconstitution (Fig. 7 E). Similarly, EC derived from Cav-1 KO mice showed loss of Ephrin-B2/Fc–induced nitric oxide production, compared with WT EC, which was rescued by Cav-1 reconstitution (Fig. 7 F). These results suggest that Eph-B4 signaling is regulated by Cav-1.

To determine if Eph-B4 signaling stimulates Cav-1 phosphorylation, we examined the effects of Ephrin-B2/Fc on EC both in vitro and in vivo. WT venous EC and venous EC derived from Eph-B4$^{+/-}$ mice were examined by FACS and Western blotting. As expected, EC derived from Eph-B4$^{+/-}$ mice showed ∼50% fewer Eph-B4 surface receptors (Fig. 8 A), as well as the presence of Myc reactivity, which is indicative of the targeted Eph-B4 deletion (Fig. 8 B). Stimulation of Eph-B4 signaling in vitro resulted in increased phosphorylation of Cav-1 on tyrosine-14 (Y14) in WT EC, compared with control EC. This tyrosine phosphorylation of Cav-1 was
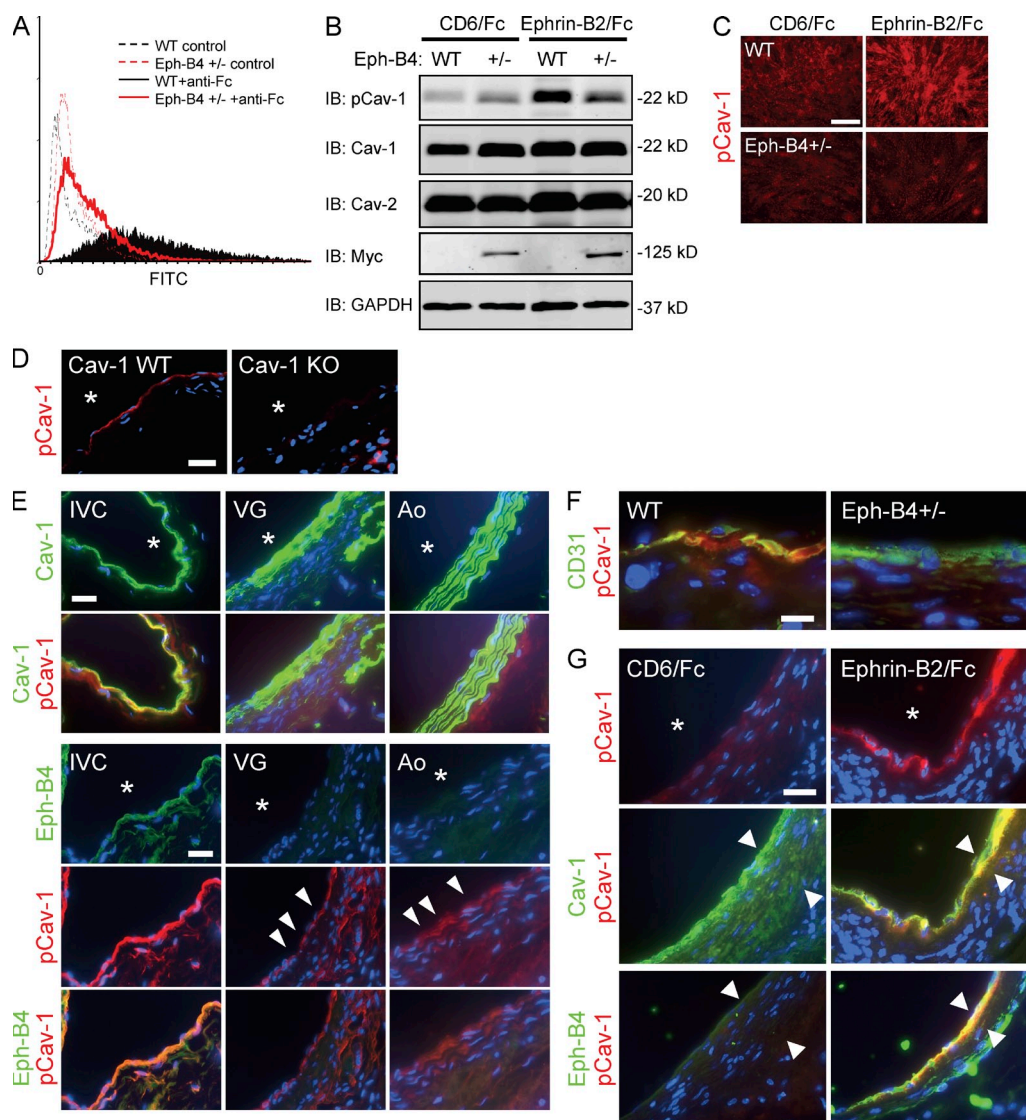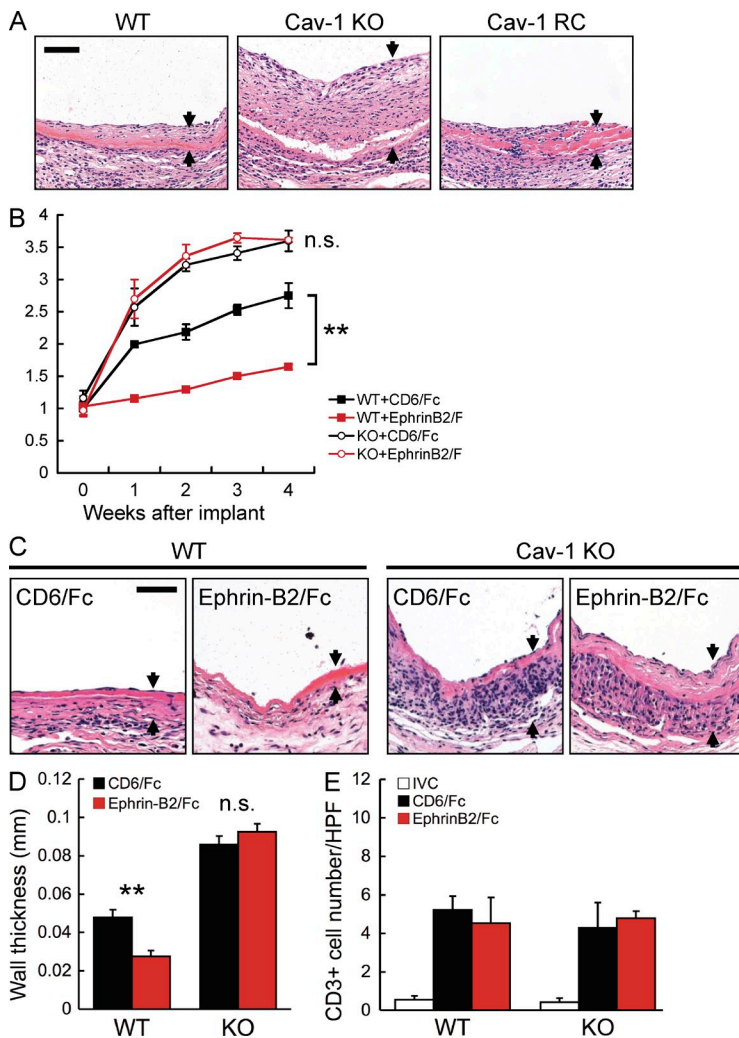
Figure 8. Eph-B4 activation stimulates Cav-1 phosphorylation in vitro and in vivo. (A) FACS analysis of venous EC derived from WT or Eph-B4^{+/−} mice. Ephrin-B2/Fc was allowed to bind to EC and then detected with anti-Fc-FITC. Control groups did not include the anti-Fc-FITC antibody. $n = 3$. (B) Phosphorylation of Cav-1 on tyrosine-14 (Y14) in WT or Eph-B4^{+/−} EC stimulated with control CD6/Fc or Ephrin-B2/Fc. $n = 3$. (C) WT or Eph-B4^{+/−} EC expression of phosphorylated-Cav-1 (red), stimulated with control CD6/Fc or Ephrin-B2/Fc. $n = 3$. Bar, 50 μm. (D) Expression in inferior vena cava (IVC) of Cav-1 WT or Cav-1 KO mice of phosphorylated Cav-1 (red). $n = 3$. Bar, 50 μm. (E) Expression in inferior vena cava, vein graft (VG), or aorta (Ao) of WT mice, of Cav-1 (green, top two rows), Eph-B4 (green, bottom three rows), phosphorylated Cav-1 (red), and both (merge). Bar, 50 μm. $n = 3$. Arrowheads denote loss of pCav-1 signal. (F) Expression in vein grafts derived from WT or Eph-B4^{+/−} mice of CD31 (green), phosphorylated Cav-1 (red), or both (merge). Counterstain is with DAPI (blue). Bar, 20 μm. $n = 3$. (G) Expression in vein grafts derived from control or Ephrin-B2/Fc–treated mice, of phosphorylated Cav-1 (red), both (merge) phosphorylated Cav-1 (red) and total Cav-1 (green), and both (merge) phosphorylated Cav-1 (red) and Eph-B4 (green). Counterstain is with DAPI (blue signal). $n = 3$. Bar, 50 μm. Arrowheads denote intimal-medial thickness. *, lumen.

reduced in EC derived from Eph-B4^{+/−} mice (Fig. 8, B and C). These results are consistent with disturbance of both Eph-B4 and Cav-1 signaling in EC derived from Eph-B4^{+/−} mice.

Eph-B4 stimulation of Cav-1 phosphorylation was also tested in vivo. As expected, Cav-1 phosphorylation was not detected in veins derived from Cav-1 KO mice (Fig. 8 D). Cav-1 was expressed in WT preimplantation veins as well as in vein grafts (3 wk) in vivo (Fig. 8 E, top row). However, similar to the reduction in Eph-B4 in vein grafts (Fig. 8 E,

third row), phosphorylated Cav-1 was reduced in vein grafts compared with preimplantation veins (Fig. 8 E, second and bottom rows). In addition, phosphorylated Cav-1 was reduced in the endothelium of vein grafts derived from Eph-B4^{+/−} mice compared with WT mice (Fig. 8 F) and increased in the endothelium of WT vein grafts treated with Ephrin-B2/Fc compared with control vein grafts (Fig. 8 G). These results suggest that Eph-B4 stimulates phosphorylation of Cav-1 in EC, both in vitro and in vein grafts in vivo. In addition,

Figure 9. Ephrin-B2/Fc inhibition of vein wall thickening depends on Cav-1. (A) Vein grafts derived from WT, homozygous Cav-1 KO mice, or Cav-1 EC-reconstituted (Cav-1 RC) mice were implanted into littermate mice, examined after 4 wk, and stained with H&E. Arrows show vein graft wall. $n = 2–7$. Bar, 50 µm. (B) Vein graft wall thickness as determined by serial ultrasounds in mice. Vein grafts were derived from WT (squares) or Cav-1 KO mice (circles) and treated with control CD6/Fc (black) or Ephrin-B2/Fc (red). $n = 5–7$. Error bars denote SEM. (C) Vein grafts were derived from WT or Cav-1 KO mice, implanted into littermate WT mice, treated with control CD6/Fc or Ephrin-B2/Fc, examined after 4 wk, and stained with H&E. Arrows show vein graft wall. $n = 5–7$. Bar, 50 µm. (D) Vein graft wall thickness in WT and Cav-1 KO vein grafts, with control CD6/Fc or Ephrin-B2/Fc treatment. $n = 5–7$. Error bars denote SEM. (E) Numbers of CD3 immunoreactive cells infiltrated into veins and vein grafts. Error bars denote SEM. $n = 5–7$. **, $P < 0.01$. n.s., not significant.

with EC-specific Cav-1 transgenic reconstitution, had greatly reduced thickness compared with vein grafts derived from Cav-1 KO mice and almost similar thickening to WT vein grafts (Fig. 9 A, right), suggesting that the thickening response is a result of endothelial Cav-1 and not global Cav-1 dysfunction.

Because Cav-1 limits vein graft thickening in a manner similar to that seen with Eph-B4 stimulation, we next determined whether Cav-1 may be a mechanism of Eph-B4–mediated vein graft adaptation. Control vein grafts implanted into littermate WT mice showed vein graft thickening that was suppressed by Ephrin-B2/Fc injection, as previously shown in Fig. 3 (Fig. 9, B [WT, red box], C [left, Ephrin-B2/Fc], and D [WT, red bar]). However, the thickened vein grafts in Cav-1 KO mice were unresponsive to Ephrin-B2/Fc injection (Fig. 9, B [KO, red circle], C [right, Ephrin-B2/Fc], and D [KO, red bar]), with similar wall thickness as the control vein grafts. There were no significant differences in CD3+ infiltrating cells in any of the vein grafts, suggesting that the thickened Cav-1 KO–derived vein grafts were not a result of T cell–mediated responses (Fig. 9 E). These results suggest that Cav-1 is downstream of Eph-B4 signaling during venous adaptation, and that Cav-1 is an effector of Eph-B4–mediated vein graft adaptation.

In WT EC, Ephrin-B2/Fc stimulation of Eph-B4 leads to receptor tyrosine phosphorylation, which then directly or indirectly interacts with Cav-1 (Fig. S4 A); however, Eph-B4 within EC derived from Cav-1 KO mice retained the ability to phosphorylate tyrosine even though Cav-1 was not detectable (Fig. S4 A). In addition, EC derived from Cav-1 KO mice did not exhibit Ephrin-B2/Fc–dependent ERK dephosphorylation, as did WT EC (Fig. S4 B), which is consistent with thicker vein grafts in veins derived from Cav-1 KO mice (Fig. 9). These results suggest that the unresponsiveness of Cav-1 KO vein grafts to Ephrin-B2/Fc treatment in vivo (Fig. 9, B [KO, red circle], C [right, Ephrin-B2/Fc], and D

these results show that phosphorylation of Cav-1 in vein grafts is correlated with Eph-B4 phosphorylation status and inversely correlated with vein graft thickness.

Cav-1 limits vein graft thickness and is a determinant of Eph-B4–mediated venous adaptation

To determine if Cav-1 is required for Eph-B4 suppression of vein graft wall thickening, we examined vein graft adaptation in WT and Cav-1 KO mice. Control vein grafts implanted into littermate WT mice showed similar vein graft thickening as that previously shown in Fig. 4 (Fig. 9 A, left). However, vein grafts derived from Cav-1 KO mice, implanted into WT hosts, showed significantly increased wall thickness (Fig. 9 A, middle), which was similar to that seen in vein grafts with reduced Eph-B4 function (Fig. 4). The increased wall thickness in vein grafts derived from Cav-1 KO mice, similar to the increased thickness of vein grafts derived from Eph-B4+/− mice, confirms our previous data that Cav-1 phosphorylation is correlated with Eph-B4 phosphorylation (Fig. 8) and also shows that Cav-1 limits vein graft thickness. In addition, vein grafts derived from Cav-1 RC mice, e.g., Cav-1 KO mice

[KO, red bar]) is specific to the interaction of Eph–B4 with Cav-1 during vein graft adaptation and not a result of the lack of Eph–B4 tyrosine phosphorylation (Fig. S5). These results also suggest that Cav-1 is a mechanism of Eph–B4 function during vein graft adaptation. Collectively, our results show that Eph–B4 phosphorylation and downstream signaling is active in adult venous EC and limits vein graft wall thickness during adaptation to the arterial environment, and that Cav-1 is an important component for this Eph–B4 function.

DISCUSSION

Using a mouse model that recapitulates aspects of human vein graft adaptation, we show that stimulation of Eph–B4 signaling is associated with vein grafts that remain morphologically thin and retain Eph–B4 protein, i.e., retain venous identity. These findings suggest that Eph–B4 remains active in normal adult veins and may promote conservation of normal venous architecture in adult tissues. Loss of Eph–B4 during venous transposition to the arterial circulation is directly responsible for loss of normal venous structure with excessive venous wall thickening and remodeling. Prevention of venous remodeling of adult vein grafts with either Ephrin–B2/Fc or adenovirus encoding WT Eph–B4 is consistent with our hypothesis that stimulation of Eph–B4 actively limits venous wall thickening. This new data suggests a function for Eph–B4 in adult veins where no such function has previously been reported. However, our findings that vein graft Eph–B4 function may be a result of endothelial Eph–B4 (Fig. 1 F and Fig. 3 B) and endothelial Cav-1 (Fig. 8 E) do not exclude the possibility that Eph–B4 function may also be present and functional in vein graft smooth muscle cells. Indeed, Eph–B4 has been reported to be present in venous smooth muscle cells (Kudo et al., 2007) and we demonstrate localization of phosphotyrosine to the media of veins treated with Ephrin–B2/Fc (Fig. 3 B). Additionally, Eph–B4 may be retained in some of the smooth muscle cells in vein grafts implanted into Ephrin–B2/Fc–treated mice (Fig. 3 H), and we show only partial recovery of thin walls in vein grafts derived from Cav-1-RC mice, i.e., mice with Cav-1 reconstituted only in the EC (Fig. 9 A). All of these data suggest that Eph–B4 signaling in vein graft smooth muscle cells may be part of the mechanism by which Eph–B4 limits venous adaptation to the arterial environment.

Veins do not form as a default pathway in response to lack of arterial expression cues. Rather, COUP-TFII expression actively determines venous identity during embryogenesis (You et al., 2005). Regardless of the upstream regulatory control mechanisms of Eph–B4 expression during embryogenesis, our findings that Eph–B4 regulates venous wall thickening in the adult shows that Eph–B4 is not simply a passive marker of venous tissue but that Eph–B4 remains functional in adult veins. As such, although the function of Eph–B4 in adult veins is not currently known, it is not surprising that regulation of venous remodeling involves Eph–B4, an RTK confined to venous tissue, and therefore may be distinct from control of arterial remodeling. Our finding that Eph–B4 expression is preserved with Ephrin–B2/Fc treatment (Fig. 3) rather than

being down–regulated suggests a novel feed-forward type of positive regulation associated with Eph–B4 and/or the venous environment. In addition, if venous adaptation to the arterial environment, that is, Eph–B4–dependent venous remodeling, is different from the response of the arterial wall to injury, then we might expect that strategies that inhibit arterial SMC proliferation and/or migration, and neointimal hyperplasia, are not effective in preventing vein graft failure, as has been reported in clinical trials (Alexander et al., 2005; Conte et al., 2006).

We also show that the activated Eph–B4 receptor is associated with Cav-1. Eph–B1 has previously been demonstrated to associate with Cav-1 (Vihanto et al., 2006), although it is not known whether compartmentalization to caveolae is a general feature of Eph receptor signaling or whether noncaveolae pools participate in cell function. However, our findings that elimination of Cav-1 abolishes vein graft thinning in response to Ephrin–B2/Fc (Fig. 9) suggest that Cav-1 is a critical mediator of Eph–B4 function during vein graft adaptation. Although we have previously demonstrated that the role of Cav-1 as a mechanosensor of physical forces lies in EC and, therefore, it is unlikely that the lack of response to Ephrin–B2/Fc reflects global caveolin dysfunction (Yu et al., 2006), the absence of Cav-1 in all cell types, and its pleotropic effects, do not exclude Cav-1 function in the vein graft smooth muscle cells.

RTKs have a highly conserved consensus sequence, $\Phi X \Phi X X X X \Phi$, where X is any amino acid and Φ is one of the aromatic acids Trp, Phe, or Tyr, which in the mouse Eph–B4 receptor is located at amino acids 804–811, near the end of the intracellular tyrosine kinase domain (amino acids 610–878) and close to the SAM domain (amino acids 911–960; Vihanto et al., 2006). Previous studies described this sequence as a putative site of interaction between Cav-1 and the RTK (García–Cardeña et al., 1997; Nystrom et al., 1999; Abulrob et al., 2004; Vihanto et al., 2006), although it is not known whether mutations of the site disrupt receptor function by prevention of protein–protein interactions, receptor phosphorylation, or perhaps other mechanisms such as subtle changes in quaternary structure (Bucci et al., 2000). Our mutated Eph–B4 plasmids and adenovirus do not undergo tyrosine phosphorylation in response to Ephrin–B2/Fc (Fig. 5, D and F; and Fig. 6 A), suggesting that both tyrosine phosphorylation and/or interaction with Cav-1 are critical aspects of Eph–B4 signaling and function during vein graft adaptation (Fig. S5). This conserved motif has previously been shown to be necessary for the catalytic function of the kinase domain and other posttranslational processing, even in the absence of direct binding of the RTK to the Cav-1 scaffolding domain (Nystrom et al., 1999). It has also been previously reported that this motif may be a place of potential interaction with Cav-1, in addition to a site of potential compartmentalization of various signaling molecules allowing rapid and selective modulation of signal transduction (Cohen et al., 2004). However, in in vitro binding studies, we could not show direct binding between Eph–B4 and Cav-1 (unpublished data), suggesting that Eph–B4 and Cav-1 interact indirectly.

Our data also shows that stimulation of Eph-B4 signaling also stimulates Cav-1 phosphorylation, both in vitro (Fig. 8, A and B) and in vivo during vein graft adaptation (Fig. 8, D–F). Although the functional significance of Cav-1 phosphorylation is not currently clearly understood, these data show that Eph-B4 and Cav-1 are linked. Because Cav-1 regulates eNOS (Fig. 7 F; Gratton et al., 2000, 2004) and NO is a regulator of vein graft wall thickness (Kibbe et al., 2001; Mayr et al., 2006), it is possible that Cav-1 mediates the effects of Eph-B4 function on vein graft wall thickness via modulation of eNOS function. The phenotype of Cav-1 KO vein grafts (Fig. 9, B–D) shows failure to remodel, which is similar to the failure of vessel remodeling in eNOS KO mice that we previously demonstrated (Rudic et al., 1998). These data suggest that both Cav-1 and eNOS are downstream mediators of Eph-B4–dependent vein graft remodeling.

We use a mouse model of venous transposition to the arterial environment that recapitulates aspects of human vein graft adaptation. In particular, certain aspects are important features of this model. The use of the inferior vena cava as a conduit allows remodeling of the vein graft to a diameter similar to that of the artery (Fig. S1, D and G). This remodeling, or change in both vessel diameter and wall thickness, is similar to the remodeling that occurs in successful human vein grafts after implantation (Owens et al., 2006, 2008). In addition, the hand-sewn anastomosis allows flexible remodeling of the anastomotic area in accordance with the main body of the vein graft, unlike the cuff anastomotic technique that is fixed and prevents remodeling. This compliance of the anastomoses allows laminar-like flow through the body of the graft with only small amounts of turbulence at the anastomoses (ultrasound data not depicted) rather than the large amounts of turbulence that are expected with the cuff technique. Lastly, the use of WT C57BL/6 mice, rather than hypercholesterolemic mice, allows us to model normal vein graft adaptation as a first understanding of vein graft responses to transplantation to the arterial environment.

In conclusion, we show that Eph-B4 is not simply a passive marker of adult veins. Rather, stimulation of Eph-B4 during vein graft adaptation promotes retention of venous identity and prevents vein wall thickening. As such, it is possible that vein graft failure may be prevented by promotion and continual stimulation of venous identity. Because Eph-B4 is a determinant of venous identity during embryogenesis, stimulation of Eph-B4 in adult cells represents a new paradigm to treat adult diseases. We believe that the success of this strategy may depend on reactivation of this differentiation program in the environmental context of loss of venous identity.

MATERIALS AND METHODS

Antibodies and reagents. Primary antibodies to the following antigens were obtained as follows: mouse Eph-B4 (R&D Systems), human Eph-B4, C4d (Lifespan), Ephrin-B2 (Neuromics), phosphotyrosine (Millipore), Cav-1, Cav-2 (BD), Cav-1, HA-tag (Santa Cruz Biotechnology, Inc.), human smooth muscle actin–HRP conjugated (Dako), F4/80 (AbD Serotec), GAPDH, Myc-Tag, phospho-histone H3, cleaved caspase-3, HA-tag (Cell Signaling Technology), RasGAP (Novus Biologicals), Ephexin-1 (ECM

Biosciences), and human IgG Fc–FITC conjugated (Sigma-Aldrich). Secondary antibodies were: biotin-conjugated anti–goat IgG and anti–mouse IgG, HRP-conjugated anti–goat IgG (Santa Cruz Biotechnology, Inc.), biotin-conjugated anti–rat IgG (Vector Laboratories), HRP-conjugated anti–rabbit IgG and anti–mouse IgG (Cell Signaling Technology), Alexa Fluor 488–, 568–, and 680–conjugated IgG (Invitrogen), and IRDye 800–conjugated IgG (Rockland). SlowFade Gold antifade reagent with DAPI (Invitrogen) was used for nuclear staining for immunofluorescence. Proteinase K (Roche), NovaRED Substrate kit, RTU horseradish peroxidase streptavidin, and DAB Substrate kits (Vector Laboratories) were used for immunohistochemistry. Recombinant mouse Ephrin-B2/Fc chimera and CD6/Fc chimera (R&D Systems) were used for stimulating the Eph-B4 receptor and the negative control, respectively.

Mouse vein graft model. All procedures, protocols, and medications were approved by the Institutional Animal Care and Use Committee and were performed and administered within National Institutes of Health and ethical guidelines. 12-wk-old C57BL/6 WT (Harlan) and EphB4$^{+/-}$ mice (The Jackson Laboratory) were purchased, and Cav-1$^{-/-}$ and Cav-1 RC mice were generated as previously described (Yu et al., 2006; Murata et al., 2007). To avoid both background effects—i.e., confounding strain-based differences in susceptibility to vein wall thickening—and potential immunological reactions from transplantation across strains, all procedures used mice that were derived from the same background as a reference group. In particular, EphB4$^{+/-}$ mice were B6.129S7 background and bred to C57BL/6 mice for two additional generations so that littermate mice were used for reference groups. Cav-1$^{-/-}$ and Cav-1 RC mice and their littermates were bred in a similar fashion, as previously described (Yu et al., 2006; Murata et al., 2007).

To obtain veins, an ∼2.0-mm segment of the intrathoracic inferior vena cava was isolated and excised. To implant the vein graft, a midline incision was made in the abdomen of a recipient mouse and the infrarenal abdominal aorta was exposed. The abdominal aorta was temporarily occluded with atraumatic micro-clamps and a segment corresponding to the length of the vein graft was excised. The vein was sutured into the arterial circulation using 10–0 nylon in continuous fashion.

Vein grafts were followed postoperatively using the Vevo770 High-Resolution Imaging System (VisualSonics). At fixed time points after surgery, mice were sacrificed to allow explantation of the vein graft. Tissue was either frozen with RNA stabilization reagent (QIAGEN) or was explanted for paraffin embedding after circulatory flushing with ice-cold PBS followed by 4% paraformaldehyde perfusion-fixation.

Vein graft wall thickness, lumen diameter, and outer wall diameter (elastic lamina) was measured in elastin-stained sections using computer morphometry (ImageJ; National Institutes of Health). The wall expansion ratio was computed by measuring the mean inner wall diameter at four points, using ultrasound, during systole and compared with that measured during diastole. The wall compliance ratio was computed by measuring, using ultrasound, the relative compliance during systole and compared with that measured during diastole.

Measurement of cell proliferation and apoptosis in vein graft sections was made by performing immunohistochemistry, using the antibodies directed against phospho-histone H3, and cleaved caspase 3, respectively. The percentage of positive cells was directly counted in at least five sections, using sections that contained at least 100 cells per field.

Ephrin-B2/Fc treatment in vivo. Both host and donor mice were treated with 20 µg of either Ephrin-B2/Fc or CD6/Fc (R&D Systems; intraperitoneal; Noren et al., 2006) starting 24 h before surgery, with additional doses given every 48 h, starting on the day after surgery, until the day before harvest. No clustering of Ephrin-B2/Fc was performed.

Construction of WT Eph-B4 and mutants of the Eph-B4 kinase domain. The cDNA sequence of mouse Eph-B4 was purchased from Open Biosystems. The Eph-B4 construct sequence was amplified by PCR with Platinum Pfx DNA polymerase (Invitrogen) using the following primers:

forward, 5′-AAACTAGTACCATGGAGCTCCGAGCGCTGCTG-3′ and reverse, 5′-CGATCGAGAACTGCTGGGCTGGTCCCCC-3′. The PCR product was prepared for insertion into the pShuttle-IRES-hrGFP-2 plasmid vector by digestion with SpeI and PvuI.

For point mutation of the Eph-B4 kinase domain (amino acid residues 804–811, sequence WSYGIVMW), the QuikChange Lightning Site-Directed Mutagenesis kit (Stratagene) was used with the following primers: w804a forward, 5′-CACCTCTGCCAGTGATGCCGCGAGCTATGGGATCGT-CATG-3′ and reverse, 5′-CATGACGATCCCATAGCTCGCGGCATC-ACTGGCAGAGGTG-3′; w811f forward, 5′-GCTATGGGATCGTCAT-GTTCGAGGTCATGTCTTTTGGG-3′ and reverse, 5′-CCCAAAAGA-CATGACCTCGAACATGACGATCCCATAGC-3′. Colonies showing uptake of the construct were screened with sequencing using the following primer: 5′-GAACTCCTCTGATCCCACCTACACAAGTTC-3′.

Eph-B4 transduction of vein grafts in vivo. First generation replication-defective adenoviruses expressing HA-tagged full-length mouse WT Eph-B4 (Ad-Eph-B4-wt), or Eph-B4 containing the mutation w804a (Ad-Eph-B4-w804a), were generated with the previously constructed plasmids using the AdEasy Adenoviral Vector System (Stratagene) and purified by cesium chloride centrifugation. The adenoviral titers were quantified by end-point dilution as previously described (Nicklin, 1999), and the MOI was calculated on the basis of the infective titer (pfu/ml).

After harvest from the donor mouse, the preimplantation vein was entirely submerged in solution with adenovirus (1.0×10^9 pfu) for 20 min on ice. After adenoviral transduction, the graft was immediately implanted into the recipient mouse as described in Mouse vein graft model. After implantation, the remainder of the adenovirus solution was mixed with pluronic gel (final concentration 20%, final volume 20 μl) and applied to the vein graft adventitia, as previously described (Kudo et al., 2007).

Cell culture. Primary cultures of mouse lung ECs (MLECs) were isolated as previously described. These ECs behave similarly to ECs derived from peripheral veins (Ackah et al., 2005). Isolated MLECs were maintained with EBM-2/EGM-2 MV SingleQuot kit Supplement & Growth Factors (Lonza) containing 15% fetal bovine serum. Human embryo kidney (HEK) 293T cells and COS cells were cultured with high-glucose Dulbecco's modified Eagle's medium supplemented with 10% fetal bovine serum.

NO release analysis. NO production by MLEC was analyzed as previously described (Fulton et al., 1999; Fernández-Hernando et al., 2006). In brief, conditioned medium was examined 0 and 24 h after Ephrin-B2/Fc treatment, without any clustering treatments. The media was processed for the measurement of nitrite (NO_2^-) by an NO-specific chemiluminescence analyzer (Sievers).

RNA extraction and RT quantitative PCR. Total RNA was isolated from cells or tissue using TRIzol Reagent (Invitrogen) and RNA was cleaned using the RNeasy Mini kit with digested DNase I (QIAGEN). For quantification of total RNA, each sample was measured using the RiboGreen RNA Assay kit (Invitrogen), and RNA quality was confirmed by the 260/280-nm ratio and random samples confirmed with 1.2% formaldehyde-agarose gel electrophoresis. RT was performed using the SuperScript III First-Strand Synthesis Supermix (Invitrogen) according to the manufacturer's instructions. Real-time quantitative PCR was performed using SYBR Green Supermix (Bio-Rad Laboratories) and amplified for 40 cycles using the iQ5 Real-Time PCR Detection system (Bio-Rad Laboratories). Correct target amplification and exclusion of nonspecific amplification was confirmed by 2% agarose gel electrophoresis, and primer efficiencies were determined by melting curve analysis. All samples were normalized by GAPDH and/or 18s RNA amplification.

Immunohistochemistry and immunofluorescence. Mouse vein graft samples were fixed as described in Mouse vein graft model. Human vein and vein graft specimens were obtained as previously described (Kudo et al, 2007). In brief, patent saphenous vein and vein grafts were explanted from

human patients undergoing cardiac transplantation, or from patients with peripheral bypass undergoing amputation for distal ischemia without infection or a thrombosed vein graft. Specimens from cardiac patients were a gift from G. Tellides (Yale University School of Medicine, New Haven, CT). Vein grafts were fixed in 10% formalin. Approval of the institutional Human Investigation Committee was obtained.

Specimens were embedded in paraffin and cut in 5-μm cross section. Hematoxylin & eosin (H&E), Masson trichrome, and van Gieson elastin staining were performed for all samples. All sections were treated for antigen retrieval using either 10 mmol/liter citrate buffer, pH 6.0 (with boiling) or 20 μg/ml proteinase K (room temperature) for 10–15 min. Cultured cells were cultured on gelatin-coated coverslips and fixed with iced methanol. No clustering treatments were performed.

Primary antibody treatment was performed according to the manufacturer's instructions and optimized concentrations where needed. For immunohistochemistry, secondary detection was performed using DAB as well as NovaRED substrate (Vector Laboratories). Sections were counterstained with Mayer's Hematoxylin. For immunofluorescence, secondary detection was performed using Alexa Fluor 488 and 568 and counterstained with DAPI. Images were captured with an AxioImager A1 (Carl Zeiss, Inc.) under identical conditions.

Immunoprecipitation. Cells were scraped with RIPA buffer supplemented with Pefabloc SC PLUS and Complete Protease Inhibitor Cocktail (Roche). Protein concentration was measured using the protein assay reagent (Bio-Rad Laboratories), and 500 μg of protein was precleared with washed protein G agarose beads (Millipore). Samples were incubated with each antibody of interest overnight at 4°C and then incubated with washed protein G agarose beads. No clustering treatments were performed. The beads were washed three times and resuspended in 50 μl Laemmli's sample buffer for final denaturation.

Sucrose gradient separation. MLEC were washed twice with PBS and scraped into ice-cold 500 mM sodium carbonate, pH 11, supplemented with 1 mg/ml protease inhibitor cocktail (Roche), dounce homogenized, and sonicated. The homogenate was then adjusted to 42.5% sucrose by the addition of 2 ml of 85% sucrose prepared in MBS (25 mM MES, pH 6.5, and 0.5 M NaCl) and placed at the bottom of an ultracentrifuge tube. A 5–30% discontinuous sucrose gradient was formed (2 ml of 5% sucrose and 6 ml of 30% sucrose, both in MES containing 250 mM sodium carbonate) and centrifuged at 35,000 rpm for 18 h. 12 1-ml gradient fractions were collected from the top, mixed with SDS/PAGE loading buffer, and equal volumes were loaded, run on the SDS/12% PAGE, and Western blotted.

Western blotting. Equal amounts of protein from each experimental group were loaded for SDS-PAGE, followed by Western blot analysis. The membranes were probed with antibodies as described in Antibodies and reagents, without any clustering treatments. Membrane signals were detected using the Odyssey infrared imaging system (LI-COR Biosciences) or the ECL detection reagent (GE Healthcare).

Cell migration. EC migration was performed using a modified Boyden chamber as previously described (Dardik et al., 2005). No clustering treatments were used.

Flow cytometry. WT and EphB4$^{+/-}$ EC were analyzed by indirect fluorescence-assisted flow cytometry. Cells were collected in cold PBS and immediately preserved with 0.5% paraformaldehyde. The cells were pretreated with Ephrin-B2/Fc to saturate surface Eph-B4 receptors, washed with cold PBS, and tagged with FITC-conjugated anti-Fc antibodies. Cells were analyzed in a flow cytometer (FACSCalibur; BD) in the FL-1 channel for FITC intensity (detected at 530 nm). Negative controls did not include the anti-Fc FITC antibody.

Statistical analysis. Results are presented as mean value ± SEM, and compared with analysis of variance. Results were considered significant when $P < 0.05$ (StatView; SAS Institute).

Online supplemental material. Fig. S1 shows morphological and physiological changes during vein graft adaptation in the mouse model. Fig. S2 shows a lack of excessive complement activation or macrophage accumulation in vein grafts derived from Ephrin-B2/Fc–treated mice. Fig. S3 shows that Cav-1 is colocalized with Eph-B4 in vivo. Fig. S4 shows that Cav-1 is not critical for Eph-B4 tyrosine phosphorylation but is important for Eph-B4 downstream signaling. Fig. S5 shows a schematic model of Cav-1 mediation of Eph-B4 downstream signaling during vein graft adaptation. Online supplemental material is available at http://www.jem.org/cgi/content/full/jem.20101854/DC1.

REFERENCES

Abeles, D., S. Kwei, G. Stavrakis, Y. Zhang, E.T. Wang, and G. García-Cardeña. 2006. Gene expression changes evoked in a venous segment exposed to arterial flow. *J. Vasc. Surg.* 44:863–870. doi:10.1016/j.jvs.2006.05.043

Abulrob, A., S. Giuseppin, M.F. Andrade, A. McDermid, M. Moreno, and D. Stanimirovic. 2004. Interactions of EGFR and caveolin-1 in human glioblastoma cells: evidence that tyrosine phosphorylation regulates EGFR association with caveolae. *Oncogene.* 23:6967–6979. doi:10.1038/sj.onc.1207911

Ackah, E., J. Yu, S. Zoellner, Y. Iwakiri, C. Skurk, R. Shibata, N. Ouchi, R.M. Easton, G. Galasso, M.J. Birnbaum, et al. 2005. Akt1/protein kinase Balpha is critical for ischemic and VEGF-mediated angiogenesis. *J. Clin. Invest.* 115:2119–2127. doi:10.1172/JCI24726

Adams, R.H., G.A. Wilkinson, C. Weiss, F. Diella, N.W. Gale, U. Deutsch, W. Risau, and R. Klein. 1999. Roles of ephrinB ligands and EphB receptors in cardiovascular development: demarcation of arterial/venous domains, vascular morphogenesis, and sprouting angiogenesis. *Genes Dev.* 13:295–306. doi:10.1101/gad.13.3.295

Alexander, J.H., G. Hafley, R.A. Harrington, E.D. Peterson, T.B. Ferguson Jr., T.J. Lorenz, A. Goyal, M. Gibson, M.J. Mack, D. Gennevois, et al; PREVENT IV Investigators. 2005. Efficacy and safety of edifoligide, an E2F transcription factor decoy, for prevention of vein graft failure following coronary artery bypass graft surgery: PREVENT IV: a randomized controlled trial. *JAMA.* 294:2446–2454. doi:10.1001/jama.294.19.2446

Bucci, M., J.P. Gratton, R.D. Rudic, L. Acevedo, F. Roviezzo, G. Cirino, and W.C. Sessa. 2000. In vivo delivery of the caveolin-1 scaffolding domain inhibits nitric oxide synthesis and reduces inflammation. *Nat. Med.* 6:1362–1367. doi:10.1038/82176

Cohen, A.W., R. Hnasko, W. Schubert, and M.P. Lisanti. 2004. Role of caveolae and caveolins in health and disease. *Physiol. Rev.* 84:1341–1379. doi:10.1152/physrev.00046.2003

Conte, M.S., D.F. Bandyk, A.W. Clowes, G.L. Moneta, L. Seely, T.J. Lorenz, H. Namini, A.D. Hamdan, S.P. Roddy, M. Belkin, et al; PREVENT III Investigators. 2006. Results of PREVENT III: a multicenter, randomized trial of edifoligide for the prevention of vein graft failure in lower extremity bypass surgery. *J. Vasc. Surg.* 43:742–751. doi:10.1016/j.jvs.2005.12.058

Couet, J., S. Li, T. Okamoto, T. Ikezu, and M.P. Lisanti. 1997a. Identification of peptide and protein ligands for the caveolin-scaffolding domain. Implications for the interaction of caveolin with caveolae-associated proteins. *J. Biol. Chem.* 272:6525–6533. doi:10.1074/jbc.272.10.6525

Couet, J., M. Sargiacomo, and M.P. Lisanti. 1997b. Interaction of a receptor tyrosine kinase, EGF-R, with caveolins. Caveolin binding negatively regulates tyrosine and serine/threonine kinase activities. *J. Biol. Chem.* 272:30429–30438. doi:10.1074/jbc.272.48.30429

Dardik, A., A. Yamashita, F. Aziz, H. Asada, and B.E. Sumpio. 2005. Shear stress-stimulated endothelial cells induce smooth muscle cell chemotaxis via platelet-derived growth factor-BB and interleukin-1alpha. *J. Vasc. Surg.* 41:321–331. doi:10.1016/j.jvs.2004.11.016

Desai, N.D., E.A. Cohen, C.D. Naylor, and S.E. Fremes; Radial Artery Patency Study Investigators. 2004. A randomized comparison of radial-artery and saphenous-vein coronary bypass grafts. *N. Engl. J. Med.* 351:2302–2309. doi:10.1056/NEJMoa040982

Erber, R., U. Eichelsbacher, V. Powajbo, T. Korn, V. Djonov, J. Lin, H.P. Hammes, R. Grobholz, A. Ullrich, and P. Vajkoczy. 2006. EphB4 controls blood vascular morphogenesis during postnatal angiogenesis. *EMBO J.* 25:628–641. doi:10.1038/sj.emboj.7600949

Fernández-Hernando, C., M. Fukata, P.N. Bernatchez, Y. Fukata, M.I. Lin, D.S. Bredt, and W.C. Sessa. 2006. Identification of Golgi-localized acyl transferases that palmitoylate and regulate endothelial nitric oxide synthase. *J. Cell Biol.* 174:369–377. doi:10.1083/jcb.200601051

Foo, S.S., C.J. Turner, S. Adams, A. Compagni, D. Aubyn, N. Kogata, P. Lindblom, M. Shani, D. Zicha, and R.H. Adams. 2006. Ephrin-B2 controls cell motility and adhesion during blood-vessel-wall assembly. *Cell.* 124:161–173. doi:10.1016/j.cell.2005.10.034

Foubert, P., J.S. Silvestre, B. Souttou, V. Barateau, C. Martin, T.G. Ebrahimian, C. Leré-Déan, J.O. Contreres, E. Sulpice, B.I. Levy, et al. 2007. PSGL-1-mediated activation of EphB4 increases the proangiogenic potential of endothelial progenitor cells. *J. Clin. Invest.* 117:1527–1537. doi:10.1172/JCI28338

Fulton, D., J.P. Gratton, T.J. McCabe, J. Fontana, Y. Fujio, K. Walsh, T.F. Franke, A. Papapetropoulos, and W.C. Sessa. 1999. Regulation of endothelium-derived nitric oxide production by the protein kinase Akt. *Nature.* 399:597–601. doi:10.1038/21218

García-Cardeña, G., P. Martasek, B.S. Masters, P.M. Skidd, J. Couet, S. Li, M.P. Lisanti, and W.C. Sessa. 1997. Dissecting the interaction between nitric oxide synthase (NOS) and caveolin. Functional significance of the nos caveolin binding domain in vivo. *J. Biol. Chem.* 272:25437–25440. doi:10.1074/jbc.272.41.25437

Gerety, S.S., H.U. Wang, Z.F. Chen, and D.J. Anderson. 1999. Symmetrical mutant phenotypes of the receptor EphB4 and its specific transmembrane ligand ephrin-B2 in cardiovascular development. *Mol. Cell.* 4:403–414. doi:10.1016/S1097-2765(00)80342-1

Gratton, J.P., J. Fontana, D.S. O'Connor, G. Garcia-Cardena, T.J. McCabe, and W.C. Sessa. 2000. Reconstitution of an endothelial nitric-oxide synthase (eNOS), hsp90, and caveolin-1 complex in vitro. Evidence that hsp90 facilitates calmodulin stimulated displacement of eNOS from caveolin-1. *J. Biol. Chem.* 275:22268–22272. doi:10.1074/jbc.M001644200

Gratton, J.P., P. Bernatchez, and W.C. Sessa. 2004. Caveolae and caveolins in the cardiovascular system. *Circ. Res.* 94:1408–1417. doi:10.1161/01.RES.0000129178.56294.17

Khot, U.N., D.T. Friedman, G. Pettersson, N.G. Smedira, J. Li, and S.G. Ellis. 2004. Radial artery bypass grafts have an increased occurrence of angiographically severe stenosis and occlusion compared with left internal mammary arteries and saphenous vein grafts. *Circulation.* 109:2086–2091. doi:10.1161/01.CIR.0000127570.20508.5C

Kibbe, M.R., E. Tzeng, S.L. Gleixner, S.C. Watkins, I. Kovesdi, A. Lizonova, M.S. Makaroun, T.R. Billiar, and R.Y. Rhee. 2001. Adenovirus-mediated gene transfer of human inducible nitric oxide synthase in porcine vein grafts inhibits intimal hyperplasia. *J. Vasc. Surg.* 34:156–165. doi:10.1067/mva.2001.113983

Kudo, F.A., A. Muto, S.P. Maloney, J.M. Pimiento, S. Bergaya, T.N. Fitzgerald, T.S. Westvik, J.C. Frattini, C.K. Breuer, C.H. Cha, et al. 2007. Venous identity is lost but arterial identity is not gained during vein graft adaptation. *Arterioscler. Thromb. Vasc. Biol.* 27:1562–1571. doi:10.1161/ATVBAHA.107.143032

Lajoie, P., E.A. Partridge, G. Guay, J.G. Goetz, J. Pawling, A. Lagana, B. Joshi, J.W. Dennis, and I.R. Nabi. 2007. Plasma membrane domain organization regulates EGFR signaling in tumor cells. *J. Cell Biol.* 179:341–356. doi:10.1083/jcb.200611106

Loftus, I.M., M.J. McCarthy, A. Lloyd, A.R. Naylor, P.R. Bell, and M.M. Thompson. 1999. Prevalence of true vein graft aneurysms: implications for aneurysm pathogenesis. *J. Vasc. Surg.* 29:403–408. doi:10.1016/S0741-5214(99)70267-3

Mann, M.J., A.D. Whittemore, M.C. Donaldson, M. Belkin, M.S. Conte, J.F. Polak, E.J. Orav, A. Ehsan, G. Dell'Acqua, and V.J. Dzau. 1999. Ex-vivo gene therapy of human vascular bypass grafts with E2F decoy: the PREVENT single-centre, randomised, controlled trial. *Lancet.* 354:1493–1498. doi:10.1016/S0140-6736(99)09405-2

Mayr, U., Y. Zou, Z. Zhang, H. Dietrich, Y. Hu, and Q. Xu. 2006. Accelerated arteriosclerosis of vein grafts in inducible NO synthase(-/-) mice is related to decreased endothelial progenitor cell repair. *Circ. Res.* 98:412–420. doi:10.1161/01.RES.0000201957.09227.6d

Murata, T., M.I. Lin, Y. Huang, J. Yu, P.M. Bauer, F.J. Giordano, and W.C. Sessa. 2007. Reexpression of caveolin-1 in endothelium rescues the vascular, cardiac, and pulmonary defects in global caveolin-1 knockout mice. *J. Exp. Med.* 204:2373–2382. doi:10.1084/jem.20062340

Nicklin, S.A. 1999. Simple methods for preparing recombinant adenovirus for high-efficiency transduction of vascular cells. *In* Vascular Disease: Molecular Biology and Gene Therapy Protocols. A.H. Baker, editor. Humana, Totowa, NJ. 271–283.

Noren, N.K., G. Foos, C.A. Hauser, and E.B. Pasquale. 2006. The EphB4 receptor suppresses breast cancer cell tumorigenicity through an Abl-Crk pathway. *Nat. Cell Biol.* 8:815–825. doi:10.1038/ncb1438

Nystrom, F.H., H. Chen, L.N. Cong, Y. Li, and M.J. Quon. 1999. Caveolin-1 interacts with the insulin receptor and can differentially modulate insulin signaling in transfected Cos-7 cells and rat adipose cells. *Mol. Endocrinol.* 13:2013–2024. doi:10.1210/me.13.12.2013

Owens, C.D., N. Wake, J.G. Jacot, M. Gerhard-Herman, P. Gaccione, M. Belkin, M.A. Creager, and M.S. Conte. 2006. Early biomechanical changes in lower extremity vein grafts—distinct temporal phases of remodeling and wall stiffness. *J. Vasc. Surg.* 44:740–746. doi:10.1016/j.jvs.2006.06.005

Owens, C.D., F.J. Rybicki, N. Wake, A. Schanzer, D. Mitsouras, M.D. Gerhard-Herman, and M.S. Conte. 2008. Early remodeling of lower extremity vein grafts: inflammation influences biomechanical adaptation. *J. Vasc. Surg.* 47:1235–1242. doi:10.1016/j.jvs.2008.01.009

Rizzo, V., D.P. McIntosh, P. Oh, and J.E. Schnitzer. 1998. In situ flow activates endothelial nitric oxide synthase in luminal caveolae of endothelium with rapid caveolin dissociation and calmodulin association. *J. Biol. Chem.* 273:34724–34729. doi:10.1074/jbc.273.52.34724

Rudic, R.D., E.G. Shesely, N. Maeda, O. Smithies, S.S. Segal, and W.C. Sessa. 1998. Direct evidence for the importance of endothelium-derived nitric oxide in vascular remodeling. *J. Clin. Invest.* 101:731–736. doi:10.1172/JCI1699

Shin, D., G. Garcia-Cardena, S. Hayashi, S. Gerety, T. Asahara, G. Stavrakis, J. Isner, J. Folkman, M.A. Gimbrone Jr., and D.J. Anderson. 2001. Expression of ephrinB2 identifies a stable genetic difference between arterial and venous vascular smooth muscle as well as endothelial cells, and marks subsets of microvessels at sites of adult neovascularization. *Dev. Biol.* 230:139–150. doi:10.1006/dbio.2000.9957

Stabila, P.F., S.C. Wong, F.A. Kaplan, and W. Tao. 1998. Cell surface expression of a human IgG Fc chimera activates macrophages through Fc receptors. *Nat. Biotechnol.* 16:1357–1360. doi:10.1038/4339

Steinle, J.J., C.J. Meininger, R. Forough, G. Wu, M.H. Wu, and H.J. Granger. 2002. Eph B4 receptor signaling mediates endothelial cell migration and proliferation via the phosphatidylinositol 3-kinase pathway. *J. Biol. Chem.* 277:43830–43835. doi:10.1074/jbc.M207221200

Szilagyi, D.E., J.P. Elliott, J.H. Hageman, R.F. Smith, and C.A. Dall'olmo. 1973. Biologic fate of autogenous vein implants as arterial substitutes: clinical, angiographic and histopathologic observations in femoro-popliteal operations for atherosclerosis. *Ann. Surg.* 178:232–246. doi:10.1097/00000658-197309000-00002

Tawara, T., K. Hasegawa, Y. Sugiura, K. Harada, T. Miura, S. Hayashi, T. Tahara, M. Ishikawa, H. Yoshida, K. Kubo, et al. 2008. Complement activation plays a key role in antibody-induced infusion toxicity in monkeys and rats. *J. Immunol.* 180:2294–2298.

Veith, F.J., S.K. Gupta, E. Ascer, S. White-Flores, R.H. Samson, L.A. Scher, J.B. Towne, V.M. Bernhard, P. Bonier, W.R. Flinn, et al. 1986. Six-year prospective multicenter randomized comparison of autologous saphenous vein and expanded polytetrafluoroethylene grafts in infrainguinal arterial reconstructions. *J. Vasc. Surg.* 3:104–114. doi:10.1067/mva.1986.avs0030104

Vihanto, M.M., C. Vindis, V. Djonov, D.P. Cerretti, and U. Huynh-Do. 2006. Caveolin-1 is required for signaling and membrane targeting of EphB1 receptor tyrosine kinase. *J. Cell Sci.* 119:2299–2309. doi:10.1242/jcs.02946

Wang, H.U., Z.F. Chen, and D.J. Anderson. 1998. Molecular distinction and angiogenic interaction between embryonic arteries and veins revealed by ephrin-B2 and its receptor Eph-B4. *Cell.* 93:741–753. doi:10.1016/S0092-8674(00)81436-1

Yamamoto, M., Y. Toya, C. Schwencke, M.P. Lisanti, M.G. Myers Jr., and Y. Ishikawa. 1998. Caveolin is an activator of insulin receptor signaling. *J. Biol. Chem.* 273:26962–26968. doi:10.1074/jbc.273.41.26962

You, L.R., F.J. Lin, C.T. Lee, F.J. DeMayo, M.J. Tsai, and S.Y. Tsai. 2005. Suppression of Notch signalling by the COUP-TFII transcription factor regulates vein identity. *Nature.* 435:98–104. doi:10.1038/nature03511

Yu, J., S. Bergaya, T. Murata, I.F. Alp, M.P. Bauer, M.I. Lin, M. Drab, T.V. Kurzchalia, R.V. Stan, and W.C. Sessa. 2006. Direct evidence for the role of caveolin-1 and caveolae in mechanotransduction and remodeling of blood vessels. *J. Clin. Invest.* 116:1284–1291. doi:10.1172/JCI27100